Article

Ion-Selective Membranes Fabricated Using Finely Controlled Swelling of Non-Ionic Fluoropolymer for Redox Flow Batteries

Fengjing Jiang [1],* and Rui Xue [2]

[1] Centre for Cooperative Research on Alternative Energies (CIC EnergiGUNE), Basque Research and Technology Alliance (BRTA), Alava Technology Park, Albert Einstein 48, 01510 Vitoria-Gasteiz, Spain
[2] ParisTech Elite Institute of Technology, Shanghai Jiao Tong University, 800 Dongchuan Rd., Shanghai 200240, China
* Correspondence: fjiang@cicenergigune.com

Abstract: Ion-selective membranes based on non-ionic polymers are promising for redox flow batteries due to their superior chemical stability and low cost. In this work, a poly(vinylidene fluoride) (PVDF) ion-selective membrane is successfully prepared using a solvent-controlled swelling method, where Nafion is used as a channel-forming promoter. The influences of Nafion on the channel formation of the membranes are studied. The results indicate that the addition of Nafion resin can greatly promote the formation of ion-conducting channels in the PVDF matrix. The obtained membranes show well-controlled proton conductivity and proton/vanadium selectivity. A battery test on a vanadium redox flow single cell is successfully performed. The energy efficiency of the cell equipped with the PVDF-based ion-selective membrane reaches 81.7% at a current density of 60 mA cm^{-2} and possesses excellent cycling stability and suppressed self-discharge after modification with Nafion.

Keywords: redox flow battery; proton conductivity; ion-selective membrane; poly(vinylidene fluoride); energy storage
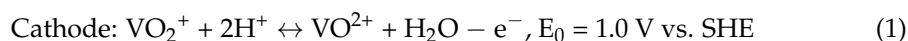
1. Introduction

The advancement toward adopting renewable energy sources in the energy transition is presently impeded by the sporadic availability of primary natural energy sources, specifically wind and solar power. The integration of a substantial proportion of these intermittent renewable resources into the electrical grid can result in grid instability, stemming from an incongruity between power generation and consumption [1,2]. Consequently, the transition to a sustainable energy system necessitates the expeditious development of dependable, high-efficiency, and economically viable energy storage technologies.

Electrochemical energy storage is one of the most important technologies for grid-scale energy storage due to its high energy efficiency and flexibility [3]. However, grid-scale energy storage has some specific requirements such as high safety, high energy efficiency, low cost, good material availability, a long charging–discharging cycling number, and a calendric life as long as 20 to 25 years. However, lithium-ion batteries have turned out to be less secure due to the risk of fire or even explosion. Furthermore, considering the huge demand of the energy storage market, the limited lithium reservation may lead to a notable increase in material cost and eventually will increase its levelized cost of storage (LCOS) [4]. Lead acid batteries have the advantages of low cost and high safety. Nevertheless, the cycling number of a lead acid battery is small and far from the requirement for large-scale energy storage. Therefore, new electrochemical technologies need to be developed to meet the requirements of large-scale energy storage.

Redox flow batteries represent a promising and innovative energy storage technology with a unique set of characteristics that make them well-suited for various applications,

including grid energy storage, renewable energy integration, and load leveling. Unlike traditional solid-state batteries, RFBs store energy in liquid electrolytes contained in separate tanks, offering scalability, flexibility, and the potential for long-duration energy storage [5–7]. Vanadium redox flow batteries (VRFBs) are the most advanced RFBs and have been considered one of the best options for grid-scale electricity storage with charge/discharge cycles over 15,000 times, short response time to load/input changes, and high round-trip energy efficiency (RTE) [6–8]. The electrolytes of all-vanadium redox flow batteries use vanadium ions in different oxidation states as active materials. Specifically, tetravalent/pentavalent vanadium serves as the cathode material, while divalent/trivalent vanadium functions as the anode material. Sulfuric acid is used as the supporting electrolyte to enhance the solubility of vanadium salts and improve proton conductivity in the electrolyte. The utilization of single vanadium as an electroactive component of the catholyte and anolyte allows for a cost-effective and straightforward means of rebalancing the electrolyte when electrolyte migration contamination occurs. This capability extends the lifespan of the vanadium electrolyte indefinitely, greatly enhancing the economic viability of all-vanadium redox flow batteries and reducing their environmental impact. Furthermore, these batteries exhibit excellent cycling stability and performance, typically achieving a stack energy efficiency of up to 85% or even higher. These factors have made all-vanadium redox flow batteries the most mature liquid flow battery technology currently available, and it has already entered the large-scale demonstration phase. The basic reactions that occur on the cathode and anode are shown as follows [9]:

$$\text{Cathode: } VO_2^+ + 2H^+ \leftrightarrow VO^{2+} + H_2O - e^-, E_0 = 1.0 \text{ V vs. SHE} \tag{1}$$

$$\text{Anode: } V^{3+} + e^- \leftrightarrow V^{2+}, E_0 = -0.26 \text{ V vs. SHE} \tag{2}$$

As a key component, the ion-selective membranes that serve as a barrier to avoid the cross-mixing of positive and negative electrolytes are one of the most expensive components of VRFBs [10,11]. The ability of the membrane to prevent the crossover of redox materials and to rapidly conduct ions directly affects the overall energy efficiency of the battery. There is a trade-off between the permeability and the proton conductivity of the membranes and optimizing both properties remains a great challenge in membrane technology. Currently, the most successfully applied proton exchange membranes (PEMs) are perfluorinated sulphonic acid polymer membranes such as Nafion® and Flemion® membranes, which can meet the requirements of high performance and low cost [12–14]. Due to their low ion-selectivity, Nafion and other cation-exchange membranes always have high vanadium ion permeation. Thus, much research work has been performed on the reduction in non-specific cation permeation [15–20]. Moreover, it was estimated that the price of Nafion membranes accounts for approximately 40% of the total cost of a VRFB cell stack [15]. Reducing the cost of ion-selective membranes is of vital importance for the development of VRFBs [21–23]. Although great efforts have been made to develop low-cost non-fluorinated polymers such as sulfonated poly (ethyl sulfone) (SPES), sulfonated polyether ether ketone (SPEEK), and polybenzimidazole (PBI), their chemical stability remains a challenge for industrial applications.

In general, nonionized polymers show advanced chemical and electrochemical stability as compared with ionic polymers having the same polymer backbone chain. The challenge with nonionic materials is that they are typically hydrophobic without adequate ion-conductive channels in the membranes and, therefore, are unfeasible for ion-conducting membranes.

Subsequently, membrane technologies for creating ion-conducting and selective channels in a nonionic membrane turn out to be challenging but meaningful. Owing to the thermal stability and chemical resistance [24], poly(vinylidene fluoride) (PVDF) has been widely studied not only in the field of fuel cells and ultrafiltration [25–27] but also for flow batteries. The PVDF/Nafion composite membrane is one of the research directions for the

application of VRFBs [28–31]. Mai et al. prepared a Nafion/PVDF blend membrane for all vanadium flow batteries, which showed an energy efficiency of 85% at a current density of 80 mA cm^{-2} with 80 wt.% of Nafion [32]. Nevertheless, a high mass ratio of Nafion was normally required in PVDF/PFSA composite membranes to maintain the high proton conductivity, which does not help much to reduce the cost.

Recently, a microporous proton-conducting membrane has attracted much attention [33–36], which utilizes the size difference between protons and other ions (particularly vanadium ions in VRFBs) to ensure the passage of H$^+$ while blocking others. W. Wei et al. prepared PVDF porous membranes using the phase inversion method [37]. J. Cao et al. investigated the improvement in a PVDF porous membrane's performance using dual coagulation [38]. These studies confirmed the promising chemical stability and feasible application of PVDF in VRFBs. However, for porous membranes possessing asymmetric structure (an ultrathin skin layer and a macro-porous supporting layer), the problem was found that the functional ultrathin skin layer serving for ion selectivity was too thin to maintain the durability of the membrane. Most of the PVDF membranes prepared using the phase inversion method possess this asymmetric structure. The thin dense layer is responsible for the ion selectivity function. Although a dense layer usually has low ion conductivity, the resistance contributed is also small due to the extremely small thickness in the range of decades of nanometers to a few micrometers.

Some research has been carried out to prepare ion-selective membranes based on nonionic polymers. However, it was found that porous membranes based on non-ionic polymers showed low ion selectivity [39].

In order to develop low-cost and durable ion-selective membranes for redox follow batteries possessing merits of low cost, chemically stable, and high performance, a novel and facile method, namely, the solvent-controlled swelling method, was invited for preparing PVDF-based ion-selective membranes, where a small amount of Nafion resin (less than 20 wt.%) was added as channel-forming promoter. Physical and electrochemical characterizations including single-cell assessments have been conducted for the evaluation of this new type of membrane.

2. Materials and Methods

2.1. Materials and Chemicals

Poly(vinylidene fluoride) (PVDF, HSV900) was produced by Arkema Co., Colombes, France. Nafion® (Dupont, D2020) was supplied by Shanghai Hesen electric Co., Ltd., Shanghai, China. Sulfuric acid (98%) and N, N-Dimethylformamide (DMF) was supplied by Lingfeng Co., Guangzhou, China. All the chemicals were used as received.

2.2. Membrane Preparation Method

Nafion was chosen as the perfluorosulfonic acid to be used as the channel-forming promoter in this work because of its excellent chemical stability, which is widely applied in vanadium redox flow batteries. A Nafion solution was prepared by replacing the low-boiling point solvent of Nafion® (Dupont, D2020) with N, N-dimethylacetamide (DMF) to obtain a 10 wt.% Nafion solution in DMF. Briefly, 18 g DMF was added to 10 g D2020 Nafion solution, followed by evaporating the low-boiling point solvent in a vacuum oven at 80 °C for 4 h, and then, additional DMF was added to the solution to obtain a 10 wt.% Nafion solution in DMF. PVDF powder was dissolved in DMF at 80 °C and stirred until the solution became homogeneous and transparent. The polymer concentration was 10–20 wt.%. The Nafion solution was added to the PVDF solution, and the mass ratio of Nafion to PVDF (pure polymer) was set as 0, 5 wt.%, 10 wt.%, and 20 wt.%, respectively. Afterward, PVDF-based ion-selective membranes were prepared using the solvent-controlled swelling method. The preparation steps are described as follows: Firstly, the casting solution containing PVDF and a small amount of Nafion resin was poured onto an even and clean glass plate to form a liquid film using a blade to control the thickness. The glass plate with the liquid film was then heated in an oven at 80 °C for 12 h to obtain a PVDF-based dense

membrane without pores or channels in the membrane. The dried membrane was then peeled off the glass plate and soaked in a swelling agent (a mixture of DMF and H_2O with a mass ratio varying from 4.7:1 to 5.3:1) for 3 h at 80 °C to construct a porous structure using controlled swelling. The porous structure, serving as the ion-conducting channels in the membrane, can be tailored by changing the swelling conditions such as the ratio of solvent to nonsolvent, the swelling temperature, and the swelling time. Finally, the obtained membranes were solidified and stabilized by immersing the swollen membrane in deionized water for 2 h at room temperature around 25 °C. When the membrane was transferred from the solvent/nonsolvent mixture into water (nonsolvent), the swelling force was quickly reduced, leading to a fast shrinking of the membrane during which the friction force between the polymer chains suddenly increased to achieve a new equilibrium. In this process, the polymer chains were immobilized, and the porous structure remained.

2.3. Characterization Methods

2.3.1. Apparent Porosity Determination of the PVDF-Based Porous Membranes

In the prepared PVDF membranes, ions can be transported via ion-conducting channels, which are formed after swelling and stabilization of the membrane. The total volume of the channels (the membrane's apparent porosity) can be evaluated by calculating the volume of absorbed water. Since the pores only exist in the swollen state, methodologies such as nitrogen adsorption isotherms and the scan electron microscope are not applicable for this purpose. For testing the water uptake, in this work, membranes were soaked in deionized water for 2 h to ensure that the membranes were fully hydrated. The mass of the fully hydrated membrane M_h was measured. After that, the membrane was completely dried, and the mass was recorded as M_d. The apparent porosity of the membrane was calculated using Equation (3):

$$\text{Porosity} = \frac{M_h - M_d}{\rho V} \tag{3}$$

where ρ is the density of water at 25 °C and V is the volume of the hydrated membrane.

2.3.2. Vanadium Ion Permeability

The diffusion coefficient of VO^{2+} was measured to evaluate the vanadium ion permeability of the membranes using the method frequently reported in the literature [16,40]. For the measurement, the testing membrane was sandwiched between two containers. One side of the testing cell was filled with a mixture of 1.5 M $VOSO_4$ and 3 M H_2SO_4, and the other side was filled with a mixture of 3 M H_2SO_4 and 1.5 M $MgSO_4$. The diffusion coefficient D of VO^{2+} was calculated according to Equation (4) [41]:

$$V_B \frac{dC_B(t)}{dt} = D\frac{A}{L}(C_A - C_B(t)) \tag{4}$$

where V_B and C_B represent the volume and VO^{2+} concentration in the vanadium-deficiency side, respectively, C_A is the concentration of VO^{2+} in the vanadium-enrichment side, A is the effective area of the testing membrane, which is 1.77 cm^2, and L is the membrane thickness.

2.3.3. Ion Conductivity and Ion Selectivity

Resistance was obtained from the Electrochemical Impedance Spectroscopy (EIS) [42] of the membranes. The testing membrane was soaked in 1.5 M H_2SO_4 for 5 h before the measurement. Ion conductivity was calculated with Equation (5):

$$\sigma = \frac{L}{A(R - R_0)} \tag{5}$$

where R and R_0 (Ω) are the measured resistances with and without the membrane and L and A represent the thickness and the area of the testing membrane, respectively. The membrane thickness was measured in the hydrated state.

Ion selectivity (S) was defined as:

$$S = \frac{\sigma}{D} \tag{6}$$

where D and σ are the diffusion coefficient of VO^{2+} and the proton conductivity of the membranes, respectively.

2.3.4. Single Cell Test

The single cell performance test was performed on a homemade flow battery cell, using a common structure. The active area (electrode area) of the VRFB single cell was 25 cm^2 (5 cm $\times$ 5 cm). Both electrodes were pretreated graphite felts specified for VRFB purchased from Liaoning Jingu Carbon Material Co., Ltd., Liaoyang, China. The original thickness of the graphite felt was around 6.0 mm, and the compressed felt was 4.0 mm thick, after being assembled. The positive electrolyte was 1.5 M V^{2+}/V^{3+}, and the negative electrolyte tank was filled with 1.5 M VO_2^+/VO^{2+} in total amount of vanadium on each side. Both electrolytes utilized 3 M H_2SO_4 as the supporting electrolyte. In total, 80 mL of each electrolyte was circulated through the half cells during the cell test. To obtain the catholyte and anolyte for the cell performance test, a V^{4+} electrolyte ($VOSO_4$) was first circulated on both sides and charged the cell to have the V^{5+} electrolyte on the positive side and the V^{3+} electrolyte on the negative side. Then, the V^{5+} electrolyte was replaced with the V^{4+} electrolyte. Therefore, the V^{4+} catholyte and V^{3+} anolyte were obtained as the starting electrolytes. The cut-off voltages were 1.65 V and 0.8 V for charging and discharging, respectively [43]. The cells were tested at various current densities ranging from 40 to 200 mA cm^{-2}. During the cycling test, the current density was maintained at 100 mA cm^{-2}. All cell tests were carried out at room temperature.

To conduct the self-discharge test, the single cells were first charged to 1.65 V at a current density of 100 mA cm^{-2} followed by being discharged to 50% of the charged capacities. Then, the open circuit voltage (OCV) was recorded as a function of time.

2.3.5. Tensile Strength

The stress–strain curves of the membranes were measured on Dynamic Thermomechanical Analysis (DMA) equipment (Q800, New Castle, DE, USA) at 25 °C with a tensile speed of 10% per minute.

2.3.6. Polarizing Micrograph

The crystalline structure of the membranes was observed with a Polarizing Microscope (DMLP, Leica, Wetzlar, Germany). This advanced microscopy system enabled us to gain profound insights into the arrangement and orientation of the crystalline components within the membranes, facilitating a comprehensive understanding of their structural properties and paving the way for further in-depth analysis and research in this field.

3. Results and Discussion

3.1. Solvent-Controlled Swelling of PVDF Ion-Selective Membranes

Swelling is a common feature of polymers, which might be one of the best methods to construct ion-conducting channels with the size of molecular level. Serious swelling of ion-exchange membranes should be avoided because excessive swelling of the membrane would make oversize ion-conducting channels and lead to insufficient ion selectivity. However, swelling itself is a facile and powerful methodology to construct ion-conducting channels in polymer membranes. Theoretically, with controlled swelling, proper proton conductivity and ion selectivity could be obtained because the diameter of the channels can be continuously adjusted at the molecular level. Herein, a solvent-controlled swelling

method is reported. The procedures of the method are schematically illustrated in Figure 1. For better control of swelling, a hydrophilic and miscible polymer with PVDF was preferred to be introduced as a channel-forming promoter. Considering the necessity of good chemical stability for real application in VRFBs, perfluorosulfonic acid, such as Nafion® membranes, turned out to be an ideal polymer. Therefore, a PVDF/Nafion-dense membrane with a small amount of Nafion was first prepared using the solution-casting method. Afterward, the dense membranes were soaked in swelling agents, which were mixtures of DMF and H_2O. By simply changing the solvent mass ratio of DMF and H_2O, the channel size of the polymer could be continuously adjusted, and thus, the ion conductivity and ion selectivity. Finally, the swollen membranes were stabilized in deionized water, during which the configuration of the polymer chains and channels was fixed. A homogeneous and transparent ion-selective PVDF-based swollen membrane is shown in Figure 2.
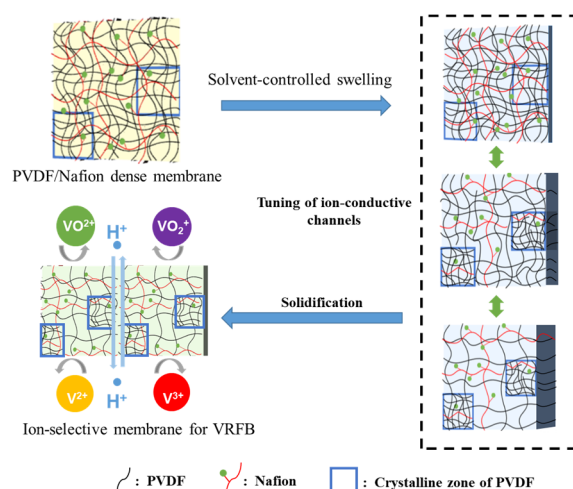
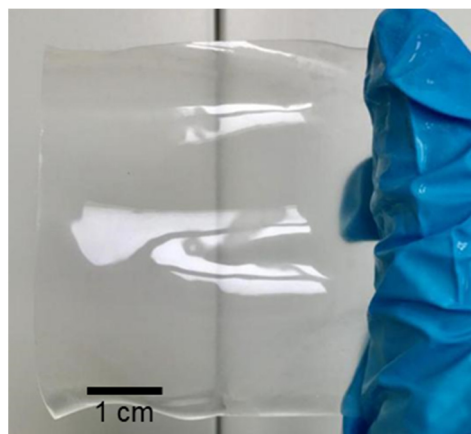**Figure 1.** Schematic diagram of the gel-solidification method.

Figure 2. Photo of the prepared PVDF-based ion-selective membrane.

3.2. Effect of Perfluorosulfonic Acid (Nafion) Content on Membrane Properties

The influence of the Nafion ratio on membrane performance was investigated. In this work, PVDF-based membranes with 0 wt.%, 5 wt.%, 10 wt.%, and 20 wt.% of Nafion were marked as PVDF, PVDF-Nafion-5, PVDF-Nafion-10, and PVDF-Nafion-20, respectively. The porosity, conductivity, and vanadium permeability of the PVDF membranes with various Nafion contents are presented in Figure 3. The membranes were swollen in the swelling agent, where the mass ratio of DMF to H_2O was 5.2:1. It can be noticed from Figure 3a that when increasing the Nafion content from 0 to 20 wt.%, there was an augment in porosity. As a result, as seen in Figure 3b and c, the proton conductivity and vanadium permeation of the membranes increased accordingly. It is worth noting

that the proton conductivity of the porous PVDF membranes is still lower than the Nafion membrane (75.3 mS cm^{-1}), and the vanadium permeability is higher than that of the Nafion membrane (2.3 × 10^{-6} cm^2 min^{-1}). The calculated ion-selectivity of the PVDF-Nafion-10 membranes was 1.21 × 10^4 S min cm^{-3}, while that of the Nafion membrane was around 3.20 × 10^4 S min cm^{-3}. Further efforts to improve the membrane conductivity and ion selectivity need to be made to perform comparable to Nafion membranes.
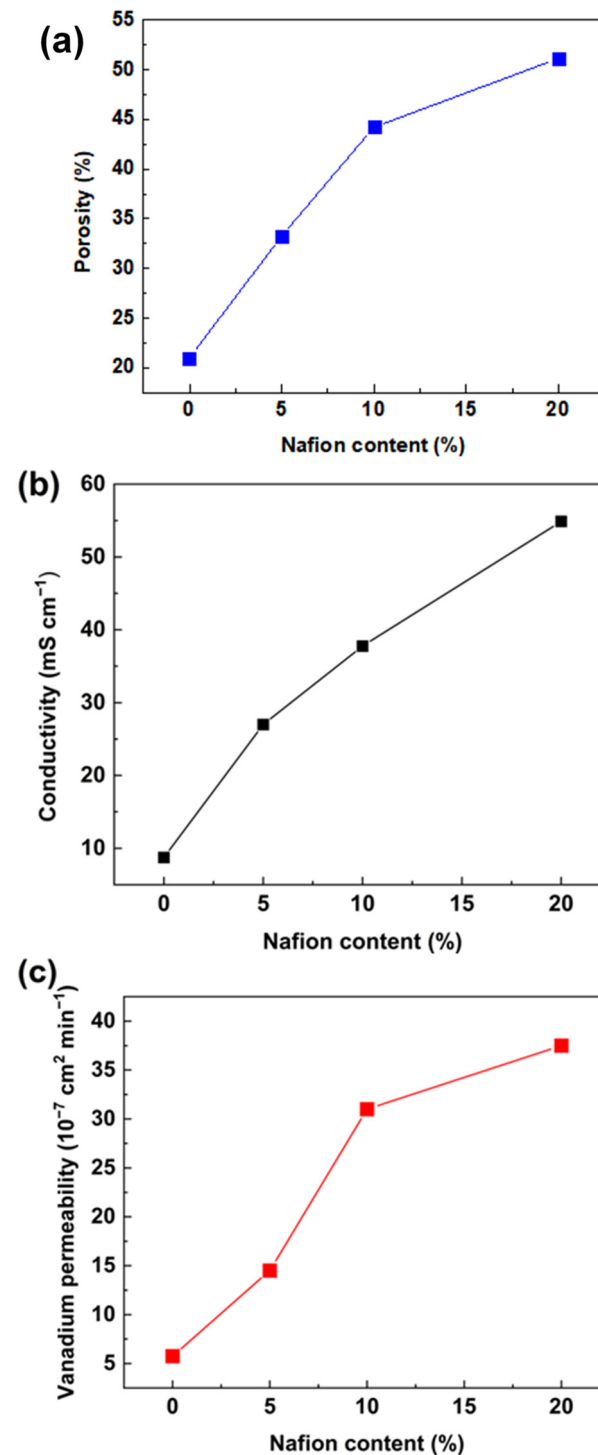
Figure 3. Influence of Nafion content on (**a**) apparent porosity, (**b**) conductivity, and (**c**) vanadium ion permeability of PVDF-based ion-selective membranes.

Polarizing micrographs are presented in Figure 4 to explain the property change in the membranes with the verifying Nafion content. All the samples were dense membranes without swelling. It can be observed that, in the PVDF, PVDF-Nafion-5, and PVDF-Nafion-10 membranes, the spherulite content of PVDF decreases with the increase in Nafion because with the small amount of Nafion mixed well with PVDF, the crystallization of PVDF was inhibited. Both the Nafion polymer and the amorphous zone of PVDF were easier to swell than the crystalline phase of PVDF [44], leading to higher channel volume (apparent porosity), proton conductivity, and ion permeability of the membranes. Note that in the PVDF-Nafion-20 membrane, the crystallinity of PVDF returned, probably because of the phase separation of Nafion and PVDF at a high Nafion ratio. In this case, the swelling of Nafion turned out to be the major reason for the further increase in porosity, proton conductivity, and ion permeability of the PVDF-Nafion-20 membrane.
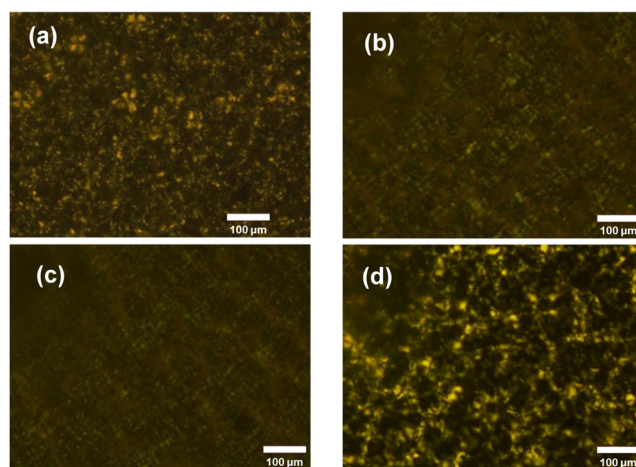

Figure 4. Polarizing micrographs of (**a**) PVDF, (**b**) PVDF-Nafion-5, (**c**) PVDF-Nafion-10, and (**d**) PVDF-Nafion-20.

3.3. Membrane Performance Tailored by the Solvent Ratio of the Swelling Agent

According to swelling theory, the swelling degree of the polymer depends largely on the solubility of the swelling agent. In order to form ion-selective channels in a PVDF membrane, the solubility of the swelling agent should be carefully adjusted. DMF is a good solvent, and H_2O is a nonsolvent for PVDF. The solubility of the mixture of DMF and H_2O could be continuously adjusted while keeping the swelling time and temperature identical. PVDF-Nafion-10 was selected as the sample membrane to study the influence of solvent ratio. The proton conductivity and permeability of the membranes treated with a solvent ratio in the range of 4.7 to 5.3 (the mass ratio of DMF to H_2O) were measured, and the results are shown in Table S1. It was found that with a solvent ratio of 4.7, the conductivity was only 13.3 mS m^{-1}, which was insufficient. On the other hand, when the solvent ratio was increased to 5.3, the proton conductivity was increased to around 55.8 mS cm^{-1}. However, the vanadium permeability could be considerably higher than that of the membrane prepared with a solvent ratio of 5.2 (3.1×10^{-6} cm^2 min^{-1}), which was not favorable for redox flow batteries. Therefore, membranes swollen with a solvent ratio of 4.8 to 5.2 were chosen for comparison in Figure 5, where the dependence of apparent porosity (a), proton conductivity (b), and vanadium ion permeability (c) on the solvent ratio of DMF to H_2O is revealed. It can be observed that when the solvent ratio increased from 4.8 to 5.2, the porosity of PVDF-Nafion-10 increased almost linearly from 36.8% to 40.6%, resulting in an increase in vanadium ion permeability from 1.2×10^{-6} cm^2 min^{-1} to 3.1×10^{-6} cm^2 min^{-1} and an enhancement in proton conductivity from 18.5 mS cm^{-1} to 37.8 mS cm^{-1}.
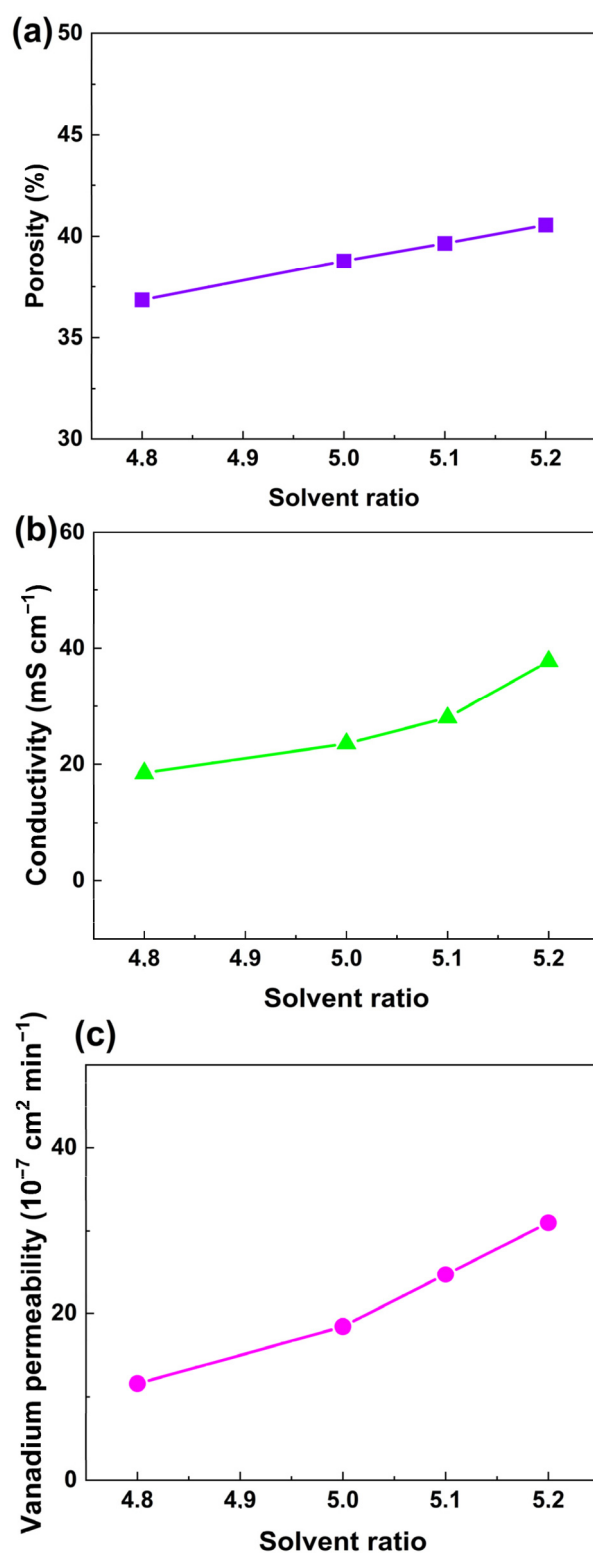
Figure 5. Dependance of (**a**) apparent porosity, (**b**) conductivity, and (**c**) vanadium ion permeability of the PVDF-based membranes on the solvent ratio of the swelling agent.

3.4. Mechanical Strength of the PVDF-Based Ion-Selective Membranes

Figure 6 illustrates the stress–strain curves of the PVDF-nafion-10 membrane with different porosities. The stress–strain curve of the solution-cast Nafion membrane was measured for comparison. The PVDF-Nafion-10 membrane swollen in the swelling agents with solvent ratios of 4.8, 5.0, and 5.2 possessed apparent porosity of 36.9%, 37.5%, and

40.6%, respectively. It can be seen from Figure 6b that as the porosity increased from 36.9% to 40.6%, the tensile strength of the membranes decreased from 19.7 MPa to 16.5 MPa, but this was still 60% higher than that of solution-cast Nafion membrane (10.7 MPa).
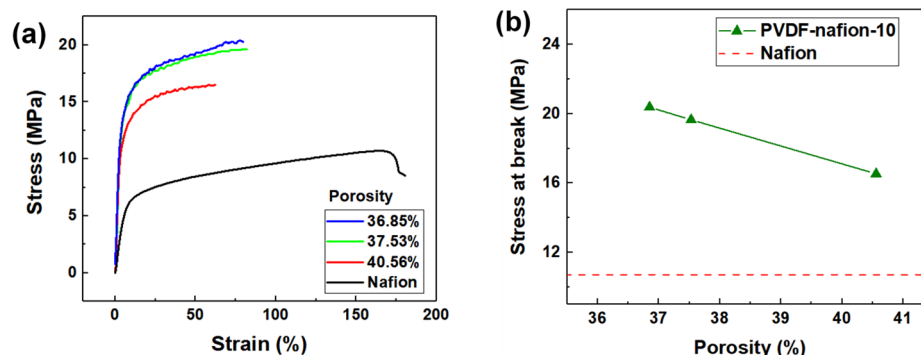

Figure 6. (**a**) Stress–strain curves and (**b**) stress at break of the PVDF-Nafion-10 membrane with various apparent porosities.

3.5. VRFB Single Cell Performance

Because of the relatively better proton conductivity, low vanadium ion permeability, and high tensile strength among the specimens, the PVDF-Nafion-10 membrane swollen with a solvent ratio of 4.8 was selected for the cell test. The proton conductivity, vanadium ion permeability, and tensile strength of the PVDF-Nafion-10 membrane were 18.5 mS cm^{-1}, 1.2×10^{-6} cm^2 min^{-1}, and 19.7 MPa, respectively. In fact, the proton conductivity of the PVDF-Nafion-10 membrane was not high when compared with that of Nafion due to the hydrophobic characteristic of the polymer matrix. However, the proton conductivity could be further increased by increasing the swelling temperature, prolonging the treatment time, or adding more solvent to the treatment mixture.

Figure 7 shows the VE, CE, and EE of the unit cell equipped with the PVDF-based membranes as a function of current density. It can be seen that the CE of the cell reached 95% and the EE of the cell reached 81.7% at 60 mA cm^{-2}. Although the cell performance of the PVDF-based swollen membranes was not yet as good as the Nation membrane, the solvent-controlled swelling method turned out to be an effective and facile approach to fabricating ion-selective membranes even with the hydrophobic PVDF membrane. For further study, efforts should be made to develop a methodology for improving the proton conductivity and ion selectivity of porous non-ionic membranes.
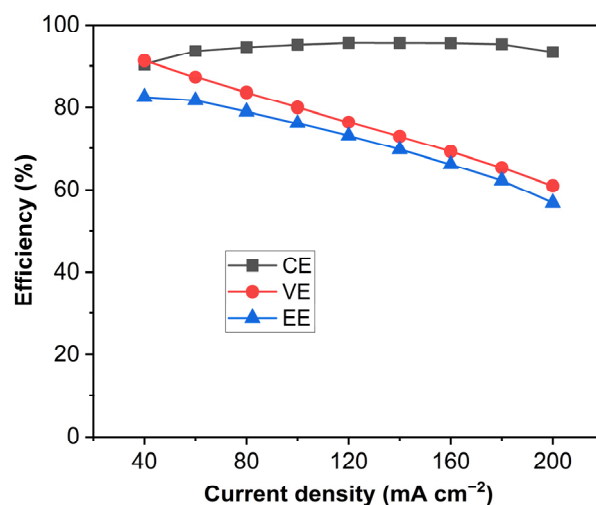

Figure 7. CE, VE, and EE of the VRFB single cell at various current densities.

In order to examine the cycling stability of the PVDF-based membrane, a test of 150 charge–discharge cycles was carried out with the same testing cell at the current density of 100 mA cm^{-2} at ambient temperatures. The results of CE, VE, and EE during the cycling test are presented in Figure 8a. The test lasted around 209 h at a constant current density of 100 mA cm^{-2}. It can be seen that the cell with the PVDF porous membrane shows stable CE, VE, and EE over the charging–discharging cycles, resulting from the excellent chemical stability of the prepared PVDF porous membrane. Furthermore, the charge and discharge capacities of the single cell were also recorded, as shown in Figure 8b. During the first 97 cycles, the charge–discharge capacity increased from 1408 mAh to 1720 mAh, probably due to the self-rebalance of the electrolyte. After the 97th cycle, the capacity decreased due to the crossover of the vanadium ions and migration of water, which is a normal phenomenon in VRFBs. It is worth noting that mainly due to the considerably lower conductivity of the sample membrane compared with the Nafion membrane, the capacity utilization of the cell was much lower (around 53%) than the normal capacity utilization of VRFB using Nafion membranes (75–85%) operated at current densities of 100 mA cm^{-2} and higher [45–47].
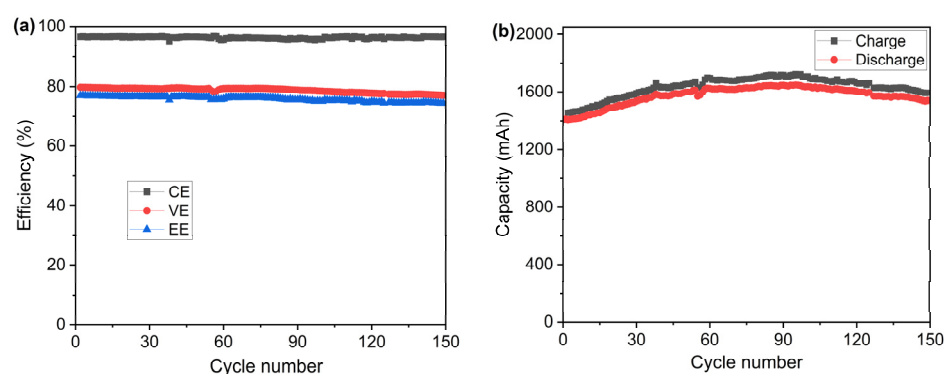

Figure 8. (**a**) Efficiency and (**b**) capacity of the VRFB single cell equipped with the porous PVDF membrane during the cycling test measured at 100 mA cm^{-2}.

The OCV curves of the PVDF-based ion-selective membranes during self-discharge as a function of time are displayed in Figure 9. All the membranes including the pure PVDF membrane were prepared using the solvent-controlled swelling method as described above. For comparison, the pure PVDF swollen membrane was adjusted to have an EE of about 81% at 60 mA cm^{-2}, which is very similar to that of the PVDF-Nafion-10 membrane. To conduct the self-discharge test, the single cells were first charged to 1.65 V at a current density of 100 mA cm^{-2}, followed by being discharged to 50% of the charged capacities, which was 709 mAh for PVDF-Nafion-10 and 607 mAh for pristine PVDF, respectively. The decline rate of the OCV of the cells was recorded to compare the rate of self-discharge resulting from vanadium ion penetration through the membrane. It can be observed that the PVDF-Nafion-10 membrane maintained an OCV above 0.8 V for more than 2900 min, while the pristine swollen PVDF membrane lasted only 1600 min, indicating significantly improved ion-selectivity by introducing Nafion into PVDF membranes. This result shows the influence of adding 10 wt.% of Nafion resin in the PVDF polymer matrix on the membrane selectivity and subsequently, the self-discharge property.
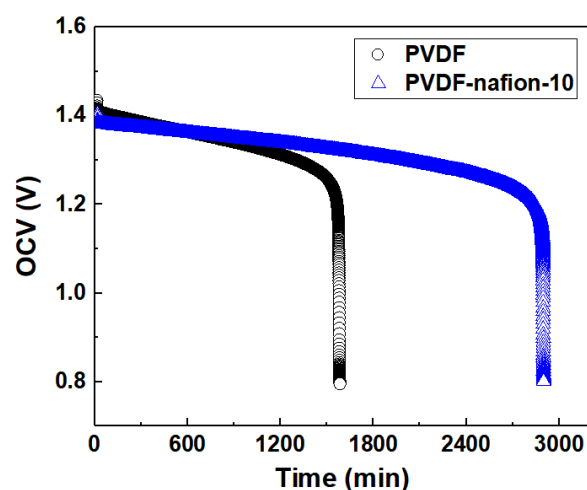
Figure 9. Self-discharge curves of PVDF-Nafion-10 and PVDF.

4. Conclusions

PVDF-based ion-selective membranes for VRFBs were successfully prepared using a solvent-controlled swelling method developed by our group. With a proper swelling solvent–nonsolvent ratio, treatment time, and temperature, the membrane turned out to be proton-conductive and efficiently ion-selective. The conductivity and selectivity of the membrane could be continuously adjusted. In addition, it was revealed that even a small amount of Nafion (10 wt%) showed a significant effect on the swelling behavior of PVDF, resulting in adjustable ion-conducting channels, proton conductivity, and vanadium ion permeability of the membranes. Moreover, by simply changing the solvent ratio of the swelling agent, the proton conductivity of the PVDF-based membrane could exceed 55 mS cm^{-2} and the vanadium permeability could be controlled at the level of 10^{-6} cm^2 min^{-1}. For the PVDF membrane containing 10 wt.% Nafion, the VRFB unit cell demonstrated an EE of 81.7% at 60 mA cm^{-2} and a much lower self-discharge rate as compared with that of the pristine swollen PVDF membrane. By inheriting the outstanding physical and chemical properties of PVDF and Nafion, the PVDF-based ion-selective membrane exhibited robust mechanical strength and excellent chemical stability. The material cost of the type of membrane could be as low as one-tenth of that of Nafion membranes. A further improvement in ion selectivity of the membrane would make the PVDF-based ion-selective membrane extremely promising for VRFBs because of the low material cost, facile membrane fabrication process, and excellent chemical stability.

References

1. Leung, P.; Li, X.; de Leon, C.P.; Berlouis, L.; Low, C.T.J.; Walsh, F.C. Progress in redox flow batteries, remaining challenges and their applications in energy storage. *RSC Adv.* **2012**, *2*, 10125–10156. [CrossRef]
2. Weber, A.Z.; Mench, M.M.; Meyers, J.P.; Ross, P.N.; Gostick, J.T.; Liu, Q. Redox flow batteries: A review. *J. Appl. Electrochem.* **2011**, *41*, 1137–1164. [CrossRef]
3. Martinez-Bolanos, J.R.; Udaeta, M.E.M.; Gimenes, A.L.V.; Silva, V.O. Economic feasibility of battery energy storage systems for replacing peak power plants for commercial consumers under energy time of use tariffs. *J. Energy Storage* **2020**, *29*, 101373. [CrossRef]
4. Darling, R.M. Techno-economic analyses of several redox flow batteries using levelized cost of energy storage. *Curr. Opin. Chem. Eng.* **2022**, *37*, 100855. [CrossRef]
5. Wang, W.; Luo, Q.; Wei, X.; Li, L.; Yang, Z. Recent Progress in Redox Flow Battery Research and Development. *Adv. Funct. Mater.* **2013**, *23*, 970–986. [CrossRef]
6. Petrov, M.M.; Modestov, A.D.; Konev, D.V.; Antipov, A.E.; Loktionov, P.A.; Pichugov, R.D.; Kartashova, N.V.; Glazkov, A.T.; Abunaeva, L.Z.; Andreev, V.N.; et al. Redox flow batteries: Role in modern electric power industry and comparative characteristics of the main types. *Russ. Chem. Rev.* **2021**, *90*, 677–702. [CrossRef]
7. Sánchez-Díez, E.; Ventosa, E.; Guarnieri, M.; Trovò, A.; Flox, C.; Marcilla, R.; Soavi, F.; Mazur, P.; Aranzabe, E.; Ferret, R. Redox flow batteries: Status and perspective towards sustainable stationary energy storage. *J. Power Sources* **2021**, *481*, 228804. [CrossRef]
8. Skyllas-Kazacos, M.; Charkarbarti, M.H.; Hajimolana, S.A.; Mjalli, F.S.; Saleem, M. Progress in Flow Battery Research and Development. *J. Electrochem. Soc.* **2011**, *158*, R55. [CrossRef]
9. Kim, K.J.; Park, M.; Kim, Y.; Kim, J.H.; Dou, S.X.; Skyllas-Kazacos, M. A technology review of electrodes and reaction mechanisms in vanadium redox flow batteries. *J. Mater. Chem.* **2015**, *3*, 16913–16933. [CrossRef]
10. Schwenzer, B.; Zhang, J.; Kim, S.; Li, L.; Liu, J.; Yang, Z. Membrane Development for Vanadium Redox Flow Batteries. *ChemSusChem* **2011**, *4*, 1388–1406. [CrossRef]
11. Zhang, Y.; Zhong, Y.; Bian, W.; Liao, W.; Zhou, X.; Jiang, F. Robust proton exchange membrane for vanadium redox flow batteries reinforced by silica-encapsulated nanocellulose. *Int. J. Hydrogen Energy* **2020**, *45*, 9803–9810. [CrossRef]
12. Mohammadi, T.; Skyllas-Kazacos, M. Preparation of sulfonated composite membrane for vanadium redox flow battery applications. *J. Membr. Sci.* **1995**, *107*, 35–45. [CrossRef]
13. Tian, B.; Yan, C.W.; Wang, F.H. Proton conducting composite membrane from Daramic/Nafion for vanadium redox flow battery. *J. Membr. Sci.* **2004**, *234*, 51–54. [CrossRef]
14. Zhang, S.; Zhang, B.; Zhao, G.; Jian, X. Anion exchange membranes from brominated poly (aryl ether ketone) containing 3, 5-dimethyl phthalazinone moieties for vanadium redox flow batteries. *J. Mater. Chem. A* **2014**, *2*, 3083–3091. [CrossRef]
15. Düerkop, D.; Widdecke, H.; Schilde, C.; Kunz, U.; Schmiemann, A. Polymer Membranes for All-Vanadium Redox Flow Batteries: A Review. *Membranes* **2021**, *11*, 214. [CrossRef]
16. Xi, J.; Wu, Z.; Qiu, X.; Chen, L. Nafion/SiO$_2$ hybrid membrane for vanadium redox flow battery. *J. Power Source* **2007**, *166*, 531–536. [CrossRef]
17. Teng, X.; Zhao, Y.; Xi, J.; Wu, Z.; Qiu, X.; Chen, L. Nafion/organically modified silicate hybrids membrane for vanadium redox flow battery. *J. Power Source* **2009**, *189*, 1240–1246. [CrossRef]
18. Jiang, F.; Kaltbeitzel, A.; Meyer, W.H.; Wegner, G. Proton-Conducting Polymers via Atom Transfer Radical Polymerization of Diisopropyl-p-Vinylbenzyl Phosphonate and 4-Vinylpyridine. *Macromolecules* **2008**, *41*, 3081–3085. [CrossRef]
19. Jiang, F.; Zhang, Y.; Tong, Y.; Yu, Q.; Hu, M. Mesoporous hollow silica spheres as micro-water-tanks in proton exchange membranes. *Polym. Test.* **2017**, *59*, 423–429. [CrossRef]
20. Schwenzer, B.; Kim, S.; Vijayakumar, M.; Yang, Z.; Liu, J. Correlation of structural differences between Nafion/polyaniline and Nafion/polypyrrole composite membranes and observed transport properties. *J. Membr. Sci.* **2011**, *372*, 11–19. [CrossRef]
21. Che, X.; Tang, W.; Dong, J.; Aili, D.; Yang, J. Anion exchange membranes based on long side-chain quaternary ammonium-functionalized poly(arylene piperidinium)s for vanadium redox flow batteries. *Sci. China Mater.* **2022**, *65*, 683–694. [CrossRef]
22. Wang, T.; Jin, Y.; Mu, T.; Wang, T.; Yang, J. Tröger's base polymer blended with poly(ether ketone cardo) for high temperature proton exchange membrane fuel cell applications. *J. Membr. Sci.* **2022**, *654*, 120539. [CrossRef]
23. Mu, T.; Leng, S.; Tang, W.; Shi, N.; Wang, G.; Yang, J. High-Performance and Low-Cost Membranes Based on Poly(vinylpyrrolidone) and Cardo-Poly(etherketone) Blends for Vanadium Redox Flow Battery Applications. *Batteries* **2022**, *8*, 230. [CrossRef]
24. Gu, M.; Zhang, J.; Wang, X.; Tao, H.; Ge, L. Formation of poly (vinylidene fluoride)(PVDF) membranes via thermally induced phase separation. *Desalination* **2006**, *192*, 160–167. [CrossRef]
25. Luo, X.; Lu, Z.; Xi, J.; Wu, Z.; Zhu, W.; Chen, L.; Qiu, X. Influences of permeation of vanadium ions through PVDF-g-PSSA membranes on performances of vanadium redox flow batteries. *J. Phys. Chem. B* **2005**, *109*, 20310–20314. [CrossRef] [PubMed]
26. Qiu, J.; Zhang, J.; Chen, J.; Peng, J.; Xu, L.; Zhai, M.; Li, J.; Wei, G. Amphoteric ion exchange membrane synthesized by radiation-induced graft copolymerization of styrene and dimethylaminoethyl methacrylate into PVDF film for vanadium redox flow battery applications. *J. Membr. Sci.* **2009**, *334*, 9–15. [CrossRef]
27. Ling, L.; Xiao, M.; Han, D.; Ren, S.; Wang, S.; Meng, Y. Porous composite membrane of PVDF/Sulfonic silica with high ion selectivity for vanadium redox flow battery. *J. Membr. Sci.* **2009**, *585*, 230–237. [CrossRef]

28. Lang, W.Z.; Xu, Z.L.; Yang, H.; Tong, W. Preparation and characterization of PVDF–PFSA blend hollow fiber UF membrane. *J. Membr. Sci.* **2007**, *288*, 123–131. [CrossRef]

29. Park, J.W.; Wycisk, R.; Pintauro, P.N. Nafion/PVDF nanofiber composite membranes for regenerative hydrogen/bromine fuel cells. *J. Membr. Sci.* **2015**, *490*, 103–112. [CrossRef]

30. Zhang, X.; Lang, W.Z.; Yan, X.; Lou, Z.; Chen, X.F. Influences of the structure parameters of multi-walled carbon nanotubes (MWNTs) on PVDF/PFSA/O-MWNTs hollow fiber ultrafiltration membranes. *J. Membr. Sci.* **2016**, *499*, 179–190. [CrossRef]

31. Zhang, X.; Shen, L.; Lang, W.Z.; Wang, Y. Improved performance of thin-film composite membrane with PVDF/PFSA substrate for forward osmosis process. *J. Membr. Sci.* **2017**, *535*, 188–199. [CrossRef]

32. Mai, Z.; Zhang, H.; Li, X.; Xiao, S.; Zhang, H. Nafion/polyvinylidene fluoride blend membranes with improved ion selectivity for vanadium redox flow battery application. *J. Power Source* **2011**, *196*, 5737–5741. [CrossRef]

33. Xue, R.; Jiang, F.; Wang, F.; Zhou, X. Towards cost-effective proton-exchange membranes for redox flow batteries: A facile and innovative method. *J. Power Source* **2020**, *449*, 227475. [CrossRef]

34. Zhou, X.; Xue, R.; Zhong, Y.; Zhang, Y.; Jiang, F. Asymmetric porous membranes with ultra-high ion selectivity for vanadium redox flow batteries. *J. Membr. Sci.* **2020**, *595*, 117614. [CrossRef]

35. Li, S.L.; Ai, X.P.; Yang, H.X.; Cao, Y.L. A polytriphenylamine-modified separator with reversible overcharge protection for 3.6 V-class lithium-ion battery. *J. Power Source* **2009**, *189*, 771–774. [CrossRef]

36. Hołda, A.K.; Vankelecom, I.F. Understanding and guiding the phase inversion process for synthesis of solvent resistant nanofiltration membranes. *J. Appl. Polym. Sci.* **2015**, *132*, 42130. [CrossRef]

37. Wei, W.; Zhang, H.; Li, X.; Zhang, H.; Li, Y.; Vankelecom, I. Hydrophobic asymmetric ultrafiltration PVDF membranes: An alternative separator for VFB with excellent stability. *Phys. Chem. Chem. Phys.* **2013**, *15*, 1766–1771. [CrossRef]

38. Cao, J.; Zhang, H.; Xu, W.; Li, X. Poly(vinylidene fluoride) porous membranes precipitated in water/ethanol dual-coagulation bath: The relationship between morphology and performance in vanadium flow battery. *J. Power Source* **2014**, *249*, 84–91. [CrossRef]

39. Shi, Y.; Eze, C.; Xiong, B.; He, W.; Zhang, H.; Lim, T.M.; Ukil, A.; Zhao, J. Recent development of membrane for vanadium redox flow battery applications: A review. *Appl. Energy* **2019**, *238*, 202–224. [CrossRef]

40. Zhang, Y.; Zhou, X.; Xue, R.; Yu, Q.; Jiang, F.; Zhong, Y. Proton exchange membranes with ultra-low vanadium ions permeability improved by sulfated zirconia for all vanadium redox flow battery. *Int. J. Hydrogen Energy* **2019**, *44*, 5997–6006. [CrossRef]

41. Luo, T.; Abdu, S.; Wessling, M. Selectivity of ion exchange membranes: A review. *J. Membr. Sci.* **2018**, *555*, 429–454. [CrossRef]

42. Zawodzinski, T.A.; Neeman, M.; Sillerud, L.O.; Gottesfeld, S. Determination of water diffusion coefficients in perfluorosulfonate ionomeric membranes. *J. Phys. Chem.* **1991**, *95*, 6040–6044. [CrossRef]

43. Derr, I.; Fetyan, A.; Schutjajew, K.; Roth, C. Electrochemical analysis of the performance loss in all vanadium redox flow batteries using different cut-off voltages. *Electrochim. Acta* **2017**, *224*, 9–16. [CrossRef]

44. Nandi, S.; Winter, H.H. Swelling behavior of partially cross-linked polymers: A ternary system. *Macromolecules* **2005**, *38*, 4447–4455. [CrossRef]

45. Jiang, H.R.; Sun, J.; Wei, L.; Wu, M.C.; Shyy, W.; Zhao, T.S. A high power density and long cycle life vanadium redox flow battery. *Energy Storage Mater.* **2020**, *24*, 529–540. [CrossRef]

46. Loktionov, P.; Pichugov, R.; Konev, D.; Petrov, M.; Pustovalova, A.; Antipov, A. Operando UV/Vis spectra deconvolution for comprehensive electrolytes analysis of vanadium redox flow battery. *J. Electroanal. Chem.* **2022**, *925*, 116912. [CrossRef]

47. Jiang, B.; Wu, L.; Yu, L.; Qiu, X.; Xi, J. A comparative study of Nafion series membranes for vanadium redox flow batteries. *J. Membr. Sci.* **2016**, *510*, 18–26. [CrossRef]